
POWER MINIMIZATION OF DOWNLINK SPECTRUM SLICING FOR eMBB AND URLLC USERS

A PREPRINT

Fabio Saggese
Dept. of Electronic System
Aalborg University
Aalborg, Denmark
fasa@es.aau.dk

Marco Moretti
Dept. of Information Engineering
University of Pisa
Pisa, Italy
marco.moretti@unipi.it

Petar Popovski
Dept. of Electronic Systems
Aalborg University
Aalborg, Denmark
petarp@es.aau.dk

Abstract

5G technology allows heterogeneous services to share the wireless spectrum within the same radio access network. In this context, *spectrum slicing* of the shared radio resources is a critical task to guarantee the performance of each service. We analyze a downlink communication serving two types of traffic: enhanced mobile broadband (eMBB) and ultra-reliable low-latency communication (URLLC). Due to the nature of low-latency traffic, the base station knows the channel state information (CSI) of the eMBB users while having statistical CSI for the URLLC users. We study the power minimization problem employing orthogonal multiple access (OMA) and non-orthogonal multiple access (NOMA) schemes. Based on this analysis, we propose a lookup table-based approach and a block coordinated descent (BCD) algorithm. We show that the BCD is optimal for the URLLC power allocation. The numerical results show that NOMA leads to lower power consumption than OMA, except when the average channel gain of the URLLC user is very high. For the latter case, the optimal approach depends on the channel condition of the eMBB user. Even when OMA attains the best performance, the gap with NOMA is negligible, showing the capability of NOMA to reduce power consumption in practically every condition.

Keywords NOMA · RAN slicing · eMBB · URLLC · Power saving

1 Introduction

The plethora of new services promised by 5G and beyond systems calls for the coexistence of very heterogeneous types of traffic on the same physical network. Some services pose strict requirements in terms of latency, others in terms of high reliability or of the huge number of devices connected to the network, while the majority of *traditional* services still require high bandwidth and data rate. To address the complexity of such a vast space of requirements, 5G standardized three generic service types: enhanced mobile broadband (eMBB), massive machine-type communications (mMTC), and ultra-reliable low-latency communications (URLLC) [1]. Note that a realistic service could require any combination of the aforementioned generic service types. At the network level, *network slicing* deals with the partitioning of the physical network infrastructure into different end-to-end isolated virtual networks able to support specific service requirements for the various use cases [2]. Similarly, at the physical layer *spectrum slicing* deals with seamlessly allocating the radio spectrum to serve users with heterogeneous requirements and is a fundamental Radio Access Network (RAN) task.

The problem of physical resource allocation for RAN slicing has been addressed in [3], where the authors allocate resource blocks (RB) to different base stations (BS) to meet the demand of mobile network operators. This work gave one of the first formalizations of the RAN slicing problem, even if it did not take into account any specific physical layer requirements. Henceforth, several works treated the problem of resource allocation algorithms to multiplex eMBB and URLLC services. In [4], the joint resource allocation problem

for eMBB-URLLC slicing is addressed by employing different puncturing models, where the reliability of the URLLC transmission is always considered met. The authors of [5] and [6] propose two deep reinforcement learning techniques to allocate resources to the two services, employing orthogonal resources and preemption/puncturing, respectively. Perfect knowledge of CSI is a crucial prerequisite for these algorithms to work properly. The authors of [7] propose a machine learning solution based on link adaptation to minimize the impact of URLLC traffic on the eMBB transmission. All these works adopt the current OMA 5G standard for dynamic resource sharing between eMBB and URLLC, either by the use of puncturing or by employing non-overlapping time/frequency resources [1]. However, NOMA has proven to outperform the OMA in many applications [8] and can also be applied to spectrum slicing, as introduced in the uplink communication framework presented in [9].

In general, most recent works on spectrum slicing for NOMA communications, such as [10]-[12], focus on the *uplink* direction because of the simpler implementation of the successive interference cancellation (SIC) strategy. The work in [10] compares the performance of NOMA and OMA for URLLC devices with different latency requirements and limited feedback by the receiver. In [11], a reinforcement learning algorithm decides whenever to use OMA or NOMA for dynamic multiplexing of eMBB-URLLC data streams, allocating the transmission power on the information of the channel state. The authors in [12] investigate the use of OMA and NOMA for intermittent and broadband services. The reliability is enforced by employing packet coding on the binary erasure channel, while the latency is modeled, taking into account reliability-latency and age of information metrics.

1.1 Contributions

In this paper, we analyze the problem of slicing the spectrum for eMBB and URLLC traffics in the *downlink* direction of a NOMA system and compare the performance with a more traditional approach based on orthogonal multiplexing. Our research addresses a simplified scenario with two users only; considering the inherent complexity of the problem, the goal of this paper is to outline the most important relationships between the two types of traffic. In an effort of abstraction, this setting, although simple, preserves all the most significant factors that affect the problem of coexistence of the eMBB and URLLC traffics in the downlink of a NOMA system.

The eMBB service aims to maximize its throughput without any latency requirements; on the contrary, the URLLC service demands mission-critical, reliable communication with a hard latency constraint. Considering the intermittent nature and the stringent latency constraints, the estimation of the instantaneous CSI is infeasible for URLLC packets, and we assume to possess only the knowledge of statistical CSI. Accordingly, the performance of the URLLC user is expressed in terms of its *outage probability*, which depends on the number of resources selected, the spectral efficiency of the transmission, and the mean signal-to-noise ratio at the receiver. On the other hand, the instantaneous CSI for the eMBB user is available, and its performance is expressed in terms of achievable rate.

With respect to the existing literature on the subject, employing a NOMA approach to the problem of downlink RAN slicing may offer significant gains but also presents many challenges. In the first place, assuming heterogeneous requirements among users dictates a new approach to SIC for NOMA. Rather than following an optimal cancellation order based on channel quality, we are constrained by the strict latency requirements of the URLLC traffic to always apply SIC at the eMBB receiver. Secondly, the propagation conditions for URLLC transmissions are so adverse due to the presence of eMBB interference and the lacking knowledge of instantaneous CSI that NOMA can be reasonably applied only in a multi-carrier approach that exploits the frequency diversity of independent parallel channels. As a consequence, the derivation of the outage probability for the URLLC traffic, similar to the problem addressed in [13] for a NOMA system with imperfect CSI, is a difficult task that can not be solved by applying the existing literature either in closed [14] or approximated form [15, 16] and requires a novel approach.

As in most scenarios where interference plays a major role, the total consumed power is a critical indicator to evaluate the performance of the system. Accordingly, we formulate the problem of eMBB-URLLC spectrum slicing with the objective of minimizing the overall power under the conflicting constraints dictated by the two types of traffic, i.e., reliable URLLC transmissions and large spectral efficiency for eMBB traffic. Numerical results investigate various aspects of the interaction of the two types of traffic and compare NOMA with OMA, the more traditional orthogonal partitioning of the radio resources. In the majority of the cases NOMA outperforms OMA being capable to reduce power consumption in practically every condition.

The main contributions of this paper can be summarized as follows:

- We propose a novel approach to downlink RAN slicing of eMBB and URLLC traffics employing non-orthogonal access technology. Slicing is formulated as a power minimization problem subject to the diverse constraints of the two types of traffic.
- To address the non-convexity of the optimization problem, we propose a novel heuristic, which follows a hierarchically layered approach: eMBB traffic is allocated first and then URLLC. This choice is motivated by a practical observation: due to the stringent latency constraints of URLLC, interference cancellation can be applied only at the eMBB receivers, which, accordingly, operate virtually in the absence of interference; for this reason, eMBB resources need to be allocated first.
- The allocation of URLLC is by far the most challenging of the two allocation problems, being plagued by the presence of the interference of the eMBB traffic and being hindered by the absence of instantaneous CSI. To address this specific problem, we propose two novel algorithms: a) a scheme based on block coordinated descent (BCD) able to converge to the optimal solution and b) a much lower-complexity strategy based on the use of lookup tables, which obtains results very close to the bound represented by the BCD scheme.
- We show by numerical simulation that in our setting NOMA outperforms OMA, i.e., that by use of NOMA we can fully exploit the frequency diversity of the system, overcoming some of the shortcomings relative to the latency requirements of the URLLC traffic.

Paper outline The remainder of the paper is organized as follows. In Section 2 the environment and the signal model are described. In the same Section, we focus also on the overall information transmittable and the possible outage events that may occur to the users. In Section 3, the allocation process is described. We firstly present the minimization power problem; then, we show how to split the problem to obtain low-complexity solutions. In Section 4, we describe the allocation strategy. Results are presented in Section 5 and conclusions in Section 6.

Mathematical notation We use capital italic letter to represent sets, e.g. \mathcal{A} , and their cardinality is denoted with capital letter, e.g. A . We denote the operator $\mathcal{A} \setminus \mathcal{B} = \{x \in \mathcal{A}, x \notin \mathcal{B}\}$. Vector are presented in bold uppercase letters \mathbf{P} ; the symbol \succeq represent the element-wise comparison between vectors. $\mathbf{1}$ and $\mathbf{0}$ are the vectors composed by ones or zeros everywhere, respectively. The symbol $\mathcal{CN}(a, B)$ represents complex Gaussian distribution with mean value a and variance B , while $\text{Exp}(a)$ represents the exponential distribution with mean value a .

2 System Model

We study a 5G-like single-cell downlink scenario. To capture the dynamics of the slicing problem, which is inherently complex, and to focus our research on the most important factors that affect the coexistence of the two types of traffic, we consider a simplified scenario composed of two users: an eMBB user, denoted by index e and a URLLC user, denoted by the index u . The available resources are organized in a time-frequency grid. In the time domain, we consider a single time slot of duration T [s]. For low-latency communications, the time slot is further divided into a set of mini-slots $\mathcal{M} = \{0, \dots, M-1\}$, $|\mathcal{M}| = M$, each one of duration $T_m = T/M$ [s]. We assume that the coherence time of the channel T_c is $T_c \geq T$ so that the channel gains can be assumed constant during an entire time slot. In the frequency domain, we consider a set $\mathcal{F} = \{0, \dots, F-1\}$, $|\mathcal{F}| = F$ of orthogonal frequency resources, each occupying a bandwidth Δ_f [Hz]. We refer to a single time-frequency resource as a *mini resource block* (mRB), where the term “mini” is used to highlight the reduced dimension in time to a conventional resource block.

The two users have different objectives and constraints: the eMBB user is modeled as transmitting a pipeline of N_e data bits per slot, while the URLLC user has to meet specific requirements in terms of latency and reliability. In detail, we assume that a packet containing N_u data bits must be delivered within T_u seconds with an outage probability lower than ϵ_u . The latency constraints are expressed as a function of the *edge delay*, i.e., the delay between the time at which the message arrives at the transmitter and the time at which the message is effectively transmitted to the user, assuming that all other delay terms have already subtracted from T_u [17]. Without loss of generality, the tolerable latency is expressed as a maximum number of mini-slots M_u^{\max} .

Resources are assigned to the users based on their traffic type (URLLC or eMBB) and the multiple access technologies adopted (OMA or NOMA). Following the 5G NR standard [1], the URLLC data transmission is allowed to span a certain number of mini-slots, due to the critical time communication. On the other

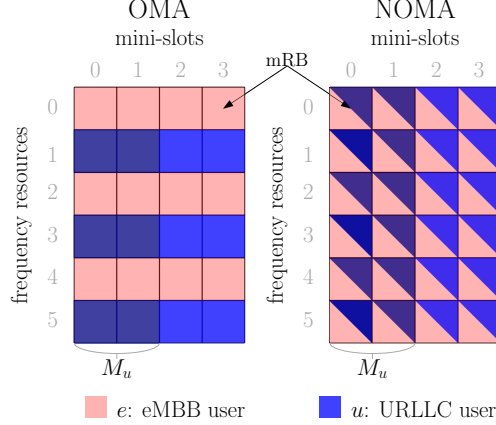


Figure 1: A toy example with a resource grid of $F = 6$ frequency channels and $M = 4$ mini-slots. In the first case, $F_u = 3$ channels, $\mathcal{F}_u = \{1, 3, 5\}$, are reserved for URLLC traffic in an OMA paradigm. In the second case, all the mRBs are reserved for u and e , i.e., $F_u = 5$ following a NOMA approach. The URLLC packet is transmitted using the first $M_u = 2$ mini-slots for both OMA and NOMA.

hand, the resource allocation for eMBB transmission can only span the entire slot, in order to support a high communication rate.

To formalize this concept, we denote as $\mathcal{F}_u \subseteq \mathcal{F}$, $|\mathcal{F}_u| = F_u$, and $\mathcal{M}_u \subseteq \mathcal{M}$, $|\mathcal{M}_u| = M_u$, the sets of frequency and temporal resources allocated for the *transmission* of the data stream of user u . It is worth noting that the URLLC tolerable latency constraints the transmission time M_u , while its F_u resources are reserved for the entire slot, i.e., for M mini-slots. We remark that this model is a generalization of other models present in the literature, which constrain the URLLC transmission to take place within a single mini-slot, i.e., imposing $M_u = 1$. When it is compatible with the latency constraints, increasing the time duration of the URLLC data transmission reduces the power needed to transmit the same amount of information. Without loss of generality, to correctly compare the schemes, we assume that only a single URLLC packet has to be served and it is transmitted immediately after its arrival.

The subset of the mRBs reserved for e is denoted as $\mathcal{F}_e \subseteq \mathcal{F}$, $|\mathcal{F}_e| = F_e$, while its set of temporal resources comprehend all the M mini-slots, as mention above. In the case of OMA, we enforce orthogonal allocation in the frequency domain, multiplexing the users on different spectral resources so that each mRB reserved for u cannot be shared with e . In the case of NOMA, all the resources reserved for e are shared with u employing different values of power to guarantee the traffic requirements of both services. Therefore, the set \mathcal{F}_e results

$$\mathcal{F}_e = \begin{cases} \mathcal{F} \setminus \mathcal{F}_u, & \text{OMA,} \\ \mathcal{F}, & \text{NOMA.} \end{cases} \quad (1)$$

An example of the resource allocation grid for both OMA and NOMA is presented in Fig. 1.

Given the number of resources assigned to each user, and being N_i the number of data bits to be transmitted for user $i \in \{e, u\}$, the average spectral efficiencies per resource [bit/s/Hz] are obtained as

$$r_u = \frac{N_u}{T_m \Delta_f F_u M_u}, \quad r_e = \frac{N_e}{T_m \Delta_f F_e M}. \quad (2)$$

Finally, the transmitter possesses different knowledge of the channel gains of the two different types of traffic. Instantaneous CSI is not available at the transmitter for URLLC traffic, and, thus, we assume that only the mean signal-to-noise ratio (SNR) Γ_u is known. On the other hand, we assume the complete knowledge of the instantaneous CSI for the eMBB user.

It is worth noting that the same model can be used when URLLC-eMBB coexistence is obtained by puncturing the eMBB data in the frequency domain. In this case, the number of mRBs given to URLLC is always $F_u = F$, while the transmission time is set to $M_u = 1$. With puncturing, the power for the eMBB service must be computed increasing the average spectral efficiency r_e , so that the eMBB data can still be recovered after erasing some part of the message. Apart from this detail, the analysis presented in the remainder of the paper is still valid also in the case of puncturing.

2.1 Signal model

We consider a multi-carrier system, where a single mRB (t, f) , corresponds to mini-slot $t \in \mathcal{M}$ and frequency resource $f \in \mathcal{F}$. Depending on the multiple access technology, each resource can be used simultaneously by both e and u users (NOMA) or by only one of them (OMA). In any case, the corresponding signals, denoted as $\mathbf{s}_e(t, f)$ for user e and as $\mathbf{s}_u(t, f)$ for user u , satisfy the following requirements

$$\mathbb{E} \{ \|\mathbf{s}_e(t, f)\|^2 \} = 1, \quad \mathbb{E} \{ \|\mathbf{s}_u(t, f)\|^2 \} = 1, \quad \mathbb{E} \{ \mathbf{s}_e^H(t, f) \mathbf{s}_u(t, f) \} = 0.$$

We remark that URLLC codewords are exactly contained in a single transmission, spanning contiguous mini-slots. In this way, if M_u is chosen appropriately, a single successful transmission carries all the information to the receiver, fulfilling the latency constraint. On the other hand, the eMBB codewords may span the whole time slot since they do not have any specific latency constraints. In the case of NOMA, the decoding process implies that one of the two users employs SIC to remove the data stream of the other (interfering) user. However, the cancellation of a user's data stream requires the reception of the entire codeword. Since eMBB codewords span an indeterminate number of mini-slots, the URLLC user that waits for the reception of the whole e codeword may incur a violation of its latency requirements. Therefore, we adopt a NOMA paradigm where *it is always the eMBB user that employs the SIC to remove the interference*, and the URLLC will always be received in the presence of the eMBB interference.

The base station (BS) transmits both eMBB and URLLC data streams using superposition coding. The transmitted signal in an mRB (t, f) is:

$$\mathbf{x}(t, f) = \sqrt{P_e(t, f)} \mathbf{s}_e(t, f) + \sqrt{P_u(t, f)} \mathbf{s}_u(t, f) \quad (3)$$

where $P_e(t, f)$, $P_u(t, f)$ are the power coefficient used to transmit the symbols of e and u on resource (t, f) , respectively. It is worth noting that this formalization implies the possibility of the transmission of the data stream of a single user $i \in \{u, e\}$ in an OMA fashion by setting the power coefficient of one of the two users equal to 0. We further denote as \mathbf{P}_e and \mathbf{P}_u the vectors collecting all the eMBB and URLLC power coefficients, respectively.

On the receiver side, we can model the signal received by user $i \in \{e, u\}$ as

$$\mathbf{y}_i(t, f) = h_i(f) \mathbf{x}(t, f) + \mathbf{n}_i \quad (4)$$

where $h_i(f)$, $i \in \{e, u\}$, is the the fading channel gain taking into account both small-scale and large-scale fading, and $n_i \sim \mathcal{N}(0, \sigma^2 \mathbf{I}_n)$, $i \in \{e, u\}$, is the noise at the receiver. Specifically, $h_e(f)$ realization is assumed known at the transmitter, while $h_u(f)$ is assumed unknown. The channel fading coefficients do not change during the whole slot. In the remainder of the paper, we assume that fading is Rayleigh distributed; however, this assumption is not essential, and all the considerations can be extended for any other kind of fading.

To simplify the notation, we further denote the normalized instantaneous SNR at the receiver $i \in \{e, u\}$ as $\gamma_i(f) = \frac{|h_i(f)|^2}{\sigma^2}$, where, for Rayleigh fading, it is $\gamma_i(f) \sim \text{Exp}(\Gamma_i)$ and $\Gamma_i = \mathbb{E}\{\gamma_i\}$, $i \in \{e, u\}$ is the normalized mean SNR at the receiver. Under the assumptions made, $\gamma_e(f)$ is known and $\gamma_u(f)$ is not known at the transmitter.

2.2 Mutual information

Due to the high number of informative bits, we can approximate the eMBB traffic to work in the infinite symbol regime, allowing for a Shannon-like information model. Due to the short packets employed for the URLLC communication, the communication is accurately described by the finite blocklength regime when the CSI is known [18]. Nevertheless, without the CSI knowledge, the finite blocklength effects disappear, as proven in [19, 20], and we can address to the outage capacity to model the communication.

According to the previous assumptions, the mutual information of u data stream at receiver u is [21]

$$I_u(\mathbf{P}_u, \mathbf{P}_e) = \frac{1}{F_u M_u} \sum_{t \in \mathcal{M}_u} \sum_{f \in \mathcal{F}_u} \log_2 \left(1 + \frac{\gamma_u(f) P_u(t, f)}{1 + \gamma_u(f) P_e(t, f)} \right); \quad [\text{bit/s/Hz}] \quad (5)$$

and the mutual information of e data stream at receiver e after a successful SIC process is

$$I_e(\mathbf{P}_e) = \frac{1}{F_e M} \sum_{t \in \mathcal{M}} \sum_{f \in \mathcal{F}_e} \log_2 (1 + \gamma_e(f) P_e(t, f)), \quad [\text{bit/s/Hz}] \quad (6)$$

where SIC process is always assumed successful in the OMA case. In the NOMA case, the SIC process can fail if the achievable rate for the u data stream at the e receiver is lower than r_u . Due to the knowledge of the e channel, the finite blocklength penalty is not zero in this case, and it depends on the required outage probability on the eMBB transmission. On the other hand, due to the relatively high value of eMBB outage probability required (e.g., 10^{-2}), the achievable rate is the 90% of the mutual information for every practical blocklength [19]. To account for the penalty, we can set $r_{u,e} = r_u/0.9$ as the target spectral efficiency to sustain for the SIC process to succeed.

The expression of the mutual information of u data stream at receiver e is

$$I_{u,e}(\mathbf{P}_u, \mathbf{P}_e) = \frac{1}{F_u M_u} \sum_{t \in \mathcal{M}_u} \sum_{f \in \mathcal{F}_u} \log_2 \left(1 + \frac{\gamma_e(f) P_u(t, f)}{1 + \gamma_e(f) P_e(t, f)} \right), \quad [\text{bit/s/Hz}] \quad (7)$$

where $I_{u,e} = 0$ in the OMA case.

2.3 Outage events

Given the mutual information denoted above, it is easy to define the outage events that may occur during the transmission towards both users.

Let us start from the outage events occurring at e . The data stream transmitted to e is incorrectly decoded if: a) SIC is not successful, or b) the data stream of e is erroneously decoded after the SIC. SIC can not be employed if $r_{u,e} > I_{u,e}$, and its probability is

$$p_{u,e}(\mathbf{P}_u, \mathbf{P}_e) = \Pr\{I_{u,e}(\mathbf{P}_u, \mathbf{P}_e) < r_{u,e}\}. \quad (8)$$

Assuming that the SIC process has been successful, the data stream of e is wrongly decoded at its own receiver if $r_e > I_e$, which occurs with probability

$$p_e(\mathbf{P}_e) = \Pr\{I_e(\mathbf{P}_e) < r_e\}. \quad (9)$$

It is worth noting that the assumption of complete knowledge of the CSI for the eMBB user constraints p_e and $p_{u,e}$ to be either 1 or 0.

Let us now focus on the outage event for u . The data stream intended for u is not successfully decoded if a) the URLLC packet is erroneously decoded at receiver u , happening if $r_u > I_u$, or b) if the URLLC packet is not entirely received before the latency requirement M_u^{\max} . Assuming the URLLC packet is transmitted as soon as it arrives, the outage probability of u can be formalized as [20]

$$p_u(\mathbf{P}_u, \mathbf{P}_e) = \Pr\{I_u(\mathbf{P}_u, \mathbf{P}_e) \leq r_u \cup M_u > M_u^{\max}\}. \quad (10)$$

Using Boole's inequality, the outage probability can be upper bound by

$$p_u(\mathbf{P}_u, \mathbf{P}_e) \leq \Pr\{I_u(\mathbf{P}_u, \mathbf{P}_e) \leq r_u\} + \Pr\{M_u > M_u^{\max}\} \quad (11)$$

which must be lower than the URLLC reliability constraint ϵ_u . The probability of the latency term in (11) can be easily constrained to be 0 by choosing a reasonable value of $M_u \leq M_u^{\max}$ so that it is

$$p_u(\mathbf{P}_u, \mathbf{P}_e) \leq \Pr\{I_u(\mathbf{P}_u, \mathbf{P}_e) \leq r_u\} \leq \epsilon_u. \quad (12)$$

According to (2), spreading the same number of informative bits on more than one mini-slot directly reduces the target rate r_u . Hence, a way to reduce the transmission power is to exploit the tolerable delay as much as possible. Nevertheless, using a large value of M_u for the transmission of a packet may prevent the prompt transmission of the following URLLC packet, increasing the latency experienced by the latter. Hence, the complete design of the transmission time should also take into account the URLLC traffic model, which is beyond the scope of this investigation. In the remainder, we address the problem of minimum power assuming M_u is given.

3 Resource allocation

We can now formalize the overall minimum power allocation problems for both OMA and NOMA schemes. We further denote as $P^{\text{tot}} = \sum_{t \in \mathcal{M}} \sum_{f \in \mathcal{F}} P_u(t, f) + P_e(t, f)$ the overall power spent.

The OMA power allocation problem is the following

$$\min_{\mathbf{P}_e, \mathbf{P}_u} P^{\text{tot}} \quad (13)$$

$$\text{s.t. } p_e(\mathbf{P}_e) = 0, \quad (13.a)$$

$$P_u(t, f)P_e(t, f) = 0, \forall t \in \mathcal{M}, \forall f \in \mathcal{F} \quad (13.b)$$

$$p_u(\mathbf{P}_u, \mathbf{P}_e = 0) \leq \epsilon_u, \quad (13.c)$$

$$\mathbf{P}_u \succeq 0, \mathbf{P}_e \succeq 0, \quad (13.d)$$

where constraint (13.a) assures that the eMBB is perfectly decoded, constraint (13.b) enforces the orthogonality of the allocation, and constraint (13.c) guarantees the reliable transmission of URLLC traffic as in (12), under the condition that $\mathbf{P}_e = 0$ due to orthogonal allocation. The NOMA allocation problem is almost identical, except for the orthogonality constraint (13.b) substituted by the SIC requirement (8), which requires that SIC is successful at the eMBB receiver. Hence, the minimization problem results

$$\min_{\mathbf{P}_e, \mathbf{P}_u} P^{\text{tot}} \quad (14)$$

$$\text{s.t. } p_e(\mathbf{P}_e) = 0, \quad (14.a)$$

$$p_{u,e}(\mathbf{P}_u, \mathbf{P}_e) = 0, \quad (14.b)$$

$$p_u(\mathbf{P}_u, \mathbf{P}_e) \leq \epsilon_u, \quad (14.c)$$

$$\mathbf{P}_u \succeq 0, \mathbf{P}_e \succeq 0, \quad (14.d)$$

Both problems are not convex w.r.t. \mathbf{P}_u and \mathbf{P}_e . In both cases, the main challenge is represented by the constraints (13.c) and (14.c) for which no known solution exists in closed form, and only bounds or approximations can be used, e.g., see [15, 16, 22]. Unfortunately, these approximations are not convex, and special functions are involved, so the optimization of the power coefficients is a hard task, even harder in the case of NOMA due to the presence of the interference. Therefore, for the NOMA scheme, where the two types of traffic interfere, we propose a heuristic based on a *layered approach* designed to decouple the allocations of the two-class of users: we first find the optimal power distribution for the eMBB and then for the URLLC users. The reason for first optimizing the eMBB allocation is the perfect knowledge of the e channel, and its transmissions are virtually interference-free, also in the NOMA scenario, since the interference can be canceled with a very high probability of success. We will show that constraints (13.c) and (14.c) can be addressed by numerical methods based on the use of look-up tables once the level of the eMBB interference is known.

We remark that practical implementation of the system should account for the maximum transmission power of the BS, which may yield an empty feasible set, i.e., no feasible solution can be found. Being interested in comparing OMA and NOMA in terms of minimum power consumed, we do not consider such power limit in problems (13) and (14), but we present experimentally the effect of imposing a power budget in Section 5.

3.1 Time-frequency selection

In the time domain, the eMBB transmission is allocated to an entire slot, as customary. Even if the URLLC could transmit on the whole time slot, its actual transmission time is constrained by the tolerable latency $M_u^{\text{max}} \geq M_u$, obtaining (12) from (11). In the frequency domain, the allocation depends on the access method selected. In the case of NOMA, all the resources are shared. Hence, the allocation sets are $\mathcal{F}_u = \mathcal{F}_e = \mathcal{F}$. In the case of OMA, we assume that the number of frequencies spanned by the URLLC transmission F_u has been selected in some way¹, resulting in knowing exactly the number of resources F_u and F_e reserved for both users. Therefore, we evaluate the frequency sets as follows. We remark that the mutual information I_e defined in (6) depends only on the power coefficients \mathbf{P}_e for both OMA and NOMA cases; therefore, it is maximized if the set \mathcal{F}_e contains the frequencies with the highest instantaneous SNR $\gamma_e(f)$ among the possible ones, or, equivalently, if the set F_u contains the mRB with lowest channel gains. Hence, the set of frequency resources given to u is

$$\mathcal{F}_u = \arg \min_{\mathcal{F}'_u \subseteq \mathcal{F}, |\mathcal{F}'_u| = F_u} \sum_{f \in \mathcal{F}'_u} \gamma_e(f), \quad (15)$$

and the set \mathcal{F}_e can be computed following (1). We remark that the mRB selection given in (15) does not influence the URLLC transmission, not knowing the CSI for those channels.

¹In Section 5 different choices of the number of frequencies are compared.

3.2 eMBB allocation

Since we have assumed that the channel is constant over the entire slot, the power allocation for eMBB, which is not affected by any interference, will be the same in every mini-slot. More formally, $P_e(t, f) = P_e(f)$, $\forall t \in \mathcal{M}$, $\forall f \in \mathcal{F}$, and (6) can be simplified in:

$$I_e(\mathbf{P}_e) = \frac{1}{F_e} \sum_{f \in \mathcal{F}_e} \log_2(1 + \gamma_e(f)P_e(f)). \quad (16)$$

Following the above assumptions, we can obtain the minimum value of eMBB power by solving

$$\min_{\mathbf{P}_e \succeq 0} \left\{ \sum_{f \in \mathcal{F}_e} P_e(f) \mid \sum_{f \in \mathcal{F}_e} \log_2(1 + \gamma_e(f)P_e(f)) \geq F_e r_e \right\}. \quad (17)$$

The solution of problem (17) can be computed through the well-known water-filling approach [21]. Coming from the general water-filling formulation [23, 24], it is easy to derive the solution providing the minimum power spent. The optimal power \mathbf{P}_e results

$$P_e(f) = \begin{cases} 2^{r_e \frac{F_e}{F_e^+}} \prod_{i \in \mathcal{F}_e^+} \left(\frac{1}{\gamma_e(i)} \right)^{\frac{1}{F_e^+}} - \frac{1}{\gamma_e(f)}, & f \in \mathcal{F}_e^+ \\ 0, & \text{otherwise} \end{cases} \quad (18)$$

where the set $\mathcal{F}_e^+ \subseteq \mathcal{F}_e$, $|\mathcal{F}_e^+| = F_e^+$, is composed by all and only the mRBs guaranteeing $P_e(f) > 0$, $\forall f \in \mathcal{F}_e^+$ [24]

Similarly, we can obtain the minimum power spent to transmit the URLLC packet satisfying the SIC requirement (14.b). The optimization problem to solve is

$$\min_{\mathbf{P}_u \succeq 0} \left\{ \sum_{f \in \mathcal{F}_u} P_u(f) \mid \sum_{f \in \mathcal{F}_u} \log_2 \left(1 + \frac{\gamma_e(f)P_u(f)}{1 + \gamma_e(f)P_e(f)} \right) \geq F_u r_{u,e} \right\}. \quad (19)$$

Also in this case, a water-filling approach may be employed considering that the normalized channels gains involved in the optimization are $\frac{\gamma_e(f)}{1 + \gamma_e(f)P_e(f)}$. The solution obtained is labeled as $\mathbf{P}_u^{\text{SIC}}$ to highlight the fact that this is the minimum power needed to satisfy the SIC constraint, whose components are

$$P_u^{\text{SIC}}(f) = \begin{cases} 2^{r_{u,e} \frac{F_u}{F_u^+}} \prod_{i \in \mathcal{F}_u^+} \left(\frac{1}{\gamma_e(i) + P_e(i)} \right)^{\frac{1}{F_u^+}} - \frac{1}{\gamma_e(f)} - P_e(f), & f \in \mathcal{F}_u^+, \\ 0, & \text{otherwise} \end{cases} \quad (20)$$

where $\mathcal{F}_u^+ \subseteq \mathcal{F}_u$, $|\mathcal{F}_u^+| = F_u^+$, collects all and only the mRBs reserved for u guaranteeing $P_u^{\text{SIC}}(f) > 0$. When we implement the OMA paradigm, we impose $\mathcal{F}_u^+ = \emptyset$, resulting in $\mathbf{P}_u^{\text{SIC}} = \mathbf{0}$.

Guaranteeing the success of SIC at the eMBB receiver, the power coefficients obtained in (20) represent the minimum value of power for u transmissions. Moreover, we remark that better eMBB channel gain conditions lead to a lower power consumption for SIC due to higher $\gamma_e(f)$ and lower $P_e(f)$ given by (18). On the other hand, when the eMBB user experiences poor channel conditions, the SIC process may be the dominant effect in the allocation of URLLC power, as we show in Section 5.

3.3 URLLC allocation

We now address the issue of optimizing the power allocation of the URLLC user under the constraint

$$p_u(\mathbf{P}_u; \mathbf{P}_e) = \Pr \{ I_u(\mathbf{P}_u; \mathbf{P}_e) \leq r_u \} \leq \epsilon_u, \quad (21)$$

where \mathbf{P}_e is now a parameter and not an optimization variable since we assume that the power coefficients for the eMBB user have already been evaluated by solution (18). As in the eMBB case, we can obtain all the power coefficients by studying a single mini-slot. The eMBB interference power coefficients depend on the frequency only, being the same for different mini-slots. Having the same interference and channel gain -

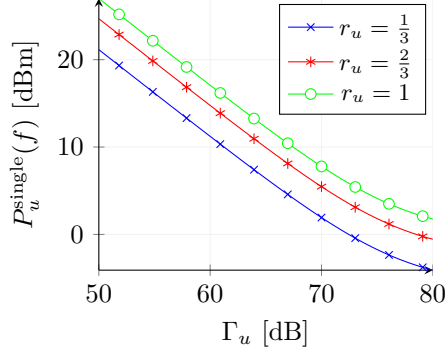


Figure 2: $P_u^{\text{single}}(f)$ as a function of Γ_u according to (24), when $\epsilon_u = 10^{-5}$ and $P_e(f) = 0$ dBm.

even if unknown - the power coefficient for URLLC transmission will depend only on the gain of the specific frequency channel, i.e. $P_u(t, f) = P_u(f)$, $t \in \mathcal{M}_u$, $f \in \mathcal{F}_u$. Thus, the mutual information I_u can be simplified in:

$$I_u(\mathbf{P}_u; \mathbf{P}_e) = \frac{1}{F_u} \sum_{f \in \mathcal{F}_u} \log_2 \left(1 + \frac{\gamma_u(f) P_u(f)}{1 + \gamma_u(f) P_e(f)} \right). \quad (22)$$

Taking into account both the constraints on the SIC process and the reliability requirement, we can now express the URLLC allocation problem as

$$\begin{aligned} \min_{\mathbf{P}_u \succeq \mathbf{P}_u^{\text{SIC}}} \quad & \sum_{f \in \mathcal{F}_u} P_u(f), \\ \text{s.t.} \quad & \Pr \left\{ \sum_{f \in \mathcal{F}_u} \log_2 \left(1 + \frac{\gamma_u(f) P_u(f)}{1 + \gamma_u(f) P_e(f)} \right) \leq F_u r_u \right\} \leq \epsilon_u. \end{aligned} \quad (23)$$

In theory, the minimization of the objective function of (23) may be obtained by applying a gradient descent approach if the chosen power coefficients always lie in the feasible set. Nevertheless, due to the unknown formulation of the outage probability, projection [25] or conditional gradient descent algorithms [26] cannot be applied directly.

In the following, we show an analytic solution of problem (23) for two particular cases: single frequency and interference-limited scenario.

3.3.1 Single frequency resource

When a single frequency resource is allocated, i.e. $F_u = 1$, the solution of (21) is known [27], and the minimum transmission power can be obtained imposing $p_u = \epsilon_u$. For a Rayleigh fading, we obtain the minimum power value on the only active frequency $f \in \mathcal{F}_u$ as

$$P_u^{\text{single}}(f) = (2^{r_u} - 1) \left(P_e(f) - \frac{1}{\Gamma_u \ln(1 - \epsilon_u)} \right). \quad (24)$$

In Fig. 2, we show $P_u^{\text{single}}(f)$ as a function of the mean normalized SNR Γ_u . The reliability is set as $\epsilon_u = 10^{-5}$ and $P_e(f) = 0$ dBm. For example, if $r_u = 1/3$, to have $P_u^{\text{single}}(f) \leq 10$ dBm we need $\Gamma_u \geq 61$ dB. Hence, transmitting on a single frequency can work only when the user experiences very good channel conditions. When $F_u > 1$, the exact evaluation of the probability presented in (21) is not known in a closed-form. Experimental results, shown in Fig. 3, obtained by Monte Carlo simulations, prove that increasing the available frequency resources will lead to a great improvement in terms of reliability. In other words, in a general case when the channel conditions are not good enough, we must rely on the diversity gain.

3.3.2 Interference-limited scenario

A bound of the power consumption for URLLC in the NOMA case can be found exploiting the asymptotic behavior with respect to $\gamma_u(f)$. When the URLLC channel conditions are very good, we can approximate

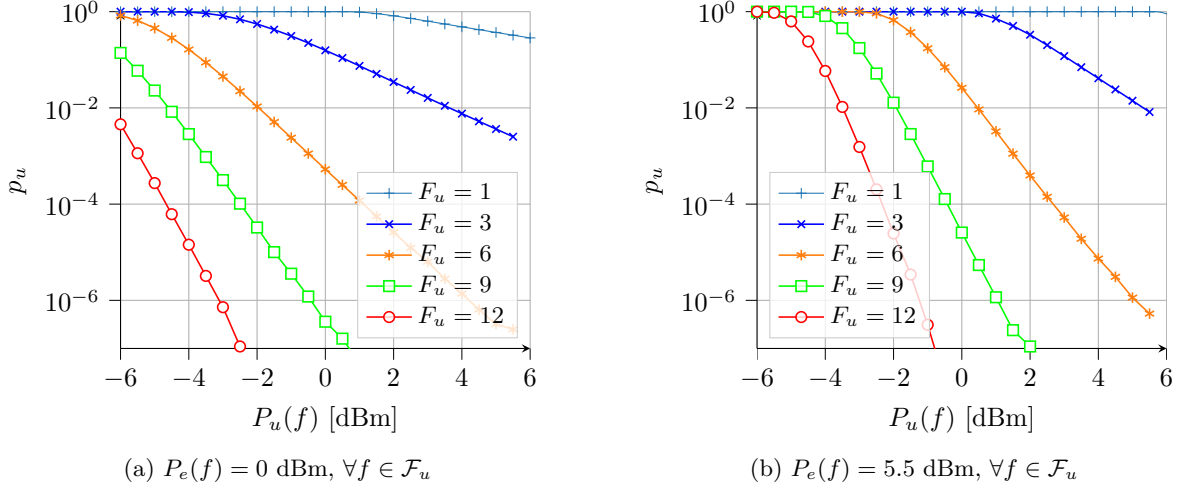


Figure 3: Experimental results of p_u (21) versus $P_u(f)$ with different number of F_u , $F_u r_u = 1$, $\Gamma_u = 30$ dB and $P_u(f) = P_u$, $\forall f \in \mathcal{F}_u$.

each term of (22) depending on the value of the interference. In detail, when the u channel gain is large, we can approximate the mutual information as

$$\log_2 \left(1 + \frac{\gamma_u(f)P_u(f)}{1 + \gamma_u(f)P_e(f)} \right) \xrightarrow{\Gamma_u \rightarrow \infty} \begin{cases} \log_2 \left(1 + \frac{P_u(f)}{P_e(f)} \right) & \text{if } P_e(f) > 0 \\ \log_2 (\gamma_u(f)P_u(f)) & \text{if } P_e(f) = 0. \end{cases} \quad (25)$$

Using the set definition given in Section 3.1, the mRBs having $P_e(f) > 0$ are collected into the set $\mathcal{F}_u \cap \mathcal{F}_e^+$, i.e., the URLLC reserved frequencies shared with \mathcal{F}_e^+ ; the mRBs having $P_e(f) = 0$ are collected in the set $\mathcal{F}_u \setminus \mathcal{F}_e^+$, i.e., the URLLC reserved frequency resources which are not in \mathcal{F}_e^+ . Therefore, for high values of Γ_u , equation (22) can be well approximated by the following

$$F_u I_u(\mathbf{P}_u; \mathbf{P}_e) \approx \sum_{f \in \mathcal{F}_u \cap \mathcal{F}_e^+} \log_2 \left(1 + \frac{P_u(f)}{P_e(f)} \right) + \sum_{f \in \mathcal{F}_u \setminus \mathcal{F}_e^+} \log_2 (\gamma_u(f)P_u(f)). \quad (26)$$

Experimental results² show that the approximation is tight for $\Gamma_u > 55$ dB.

The summation of terms involving no interference leads to a formulation of the outage probability, which can be tightly bounded using the approach given in [15]. However, this bound is still very complicated depending on special functions, while we are interested in a simple formulation suggesting the behavior of the power allocation for the interference-limited case. To overcome this, we note that the term where $P_e(f) > 0$ has a high probability of being greater than the biggest term where $P_e(f) = 0$. In other words, if we consider the mRB with the lowest interference greater than 0, i.e., $f^{\min} = \arg \min_{f \in \mathcal{F}_u \cap \mathcal{F}_e^+} P_e(f)$, the probability that each realization of the SNR in $\mathcal{F}_u \setminus \mathcal{F}_e^+$ is greater than the lowest interference is

$$\prod_{f \in \mathcal{F}_u \setminus \mathcal{F}_e^+} \Pr \left\{ \gamma_u(f) \geq \frac{1}{P_e(f^{\min})} \right\} = e^{-\frac{|\mathcal{F}_u \setminus \mathcal{F}_e^+|}{\Gamma_u P_e(f^{\min})}} \xrightarrow{\Gamma_u \rightarrow \infty} 1, \quad (27)$$

for i.i.d. Rayleigh fading. Therefore, we can substitute $1/P_e(f^{\min})$ to all the channels experiencing no interference $\mathcal{F}_u \setminus \mathcal{F}_e^+$. In this way, we obtain an approximate formulation which is a lower bound of (26) almost surely.

To summarize, when the system is interference-limited, equation (22) is bounded with high probability by

$$I_u(\mathbf{P}_u; \mathbf{P}_e) \geq \tilde{I}_u(\mathbf{P}_u; \mathbf{P}_e) = \frac{1}{F_u} \sum_{f \in \mathcal{F}_u} \log_2 \left(1 + \frac{P_u(f)}{P_e(f)} \right), \quad (28)$$

where it is implied that $P_e(f) = P_e(f^{\min})$, $\forall f \in \mathcal{F}_u \setminus \mathcal{F}_e^+$. Hence, finding the power coefficients \mathbf{P}_u guaranteeing $\tilde{I}_u(\mathbf{P}_u; \mathbf{P}_e) \geq r_u$, we obtain that $\Pr\{I_u(\mathbf{P}_u); \mathbf{P}_e \geq r_u\} \rightarrow 1$.

²The results are easily reproducible from expression (26), but not provided for lack of space.

Using (28), the minimum power coefficients can be found solving the following problem

$$\min_{\mathbf{P}_u \geq 0} \left\{ \sum_{f \in \mathcal{F}_u} P_u(f) \mid \sum_{f \in \mathcal{F}_u} \log_2 \left(1 + \frac{P_u(f)}{P_e(f)} \right) \geq F_u r_u \right\}. \quad (29)$$

Using the water-filling approach, setting the channel gain of each mRB as $1/P_e(f)$, we obtain

$$P_u^{\text{IL}}(f) = \begin{cases} 2^{r_u F_u} \prod_{i \in \mathcal{F}_u} P_e(i)^{\frac{1}{F_u}} - P_e(f), & f \in \mathcal{F}_u, \\ 0, & \text{otherwise.} \end{cases} \quad (30)$$

Solution (30) leads to a vector \mathbf{P}_u^{IL} which guarantees that $\tilde{I}_u(\mathbf{P}_u^{\text{IL}}; \mathbf{P}_e) \geq r_u$ for the interference-limited scenario. In the numerical results, we show that the interference-limited scenario may occur when the eMBB user is the farther user. In this kind of scenarios, \mathbf{P}_u^{IL} (30) can be used efficiently for the URLLC allocation.

4 Simplified solutions for power allocation

Even if a closed-form for computing the power (21) does not exist, we may state a non-increasing property of the outage probability, which is useful for the proposed simplified solutions.

Proposition 1. *Assuming fixed values of r_u , and \mathbf{P}_e , the outage probability (21) is a non-increasing monotone function of \mathbf{P}_u .*

Proof. See Appendix A. □

4.1 A lookup table estimation of URLLC outage probability

To estimate the outage probability, we will make use of a lookup table based on Monte Carlo simulations. From (21), the outage probability depends on the value of several parameters: r_u , Γ_u , \mathcal{F}_u , \mathbf{P}_e and \mathbf{P}_u . In theory, we can tabulate the outage probability with a specific entry for each of these parameters. However, populating the table for all the possible vectors \mathbf{P}_e and \mathbf{P}_u will require an extremely large number of trials and a huge dimension of the table itself. Furthermore, the complexity increases with the number of channels \mathcal{F}_u employed, obtaining even bigger tables for greater frequency sets. To overcome all these problems, we tabulate the outage probability assuming that the same values of P_u and the same values of P_e are used on all the considered mRBs. Let us denote as

$$\hat{p}_u(P_u, P_e, \Gamma_u, \mathcal{F}_u, r_u) = \lim_{n \rightarrow \infty} \frac{1}{n} \sum_{i=1}^n \mathbb{1} \left\{ \sum_{f \in \mathcal{F}_u} \log \left(1 + \frac{P_u \gamma_u(f)}{1 + P_e \gamma_u(f)} \right) \leq F_u r_u \right\} \quad (31)$$

the Monte Carlo estimation of the outage probability p_u when $P_u(f) = P_u$ and $P_e(f) = P_e \forall f \in \mathcal{F}_u$, where $\mathbb{1}\{\cdot\}$ is the indicator function. The number of elements of the table is denoted as L and depends on the quantity of parameters under test for power, frequency, SNR, and spectral efficiency values. From now on, we will recall eq. (31) to address the whole lookup table for simplicity.

4.2 A lookup table-based feasible algorithm for power allocation

Both allocation problems (13) and (14) can be solved following a sequential algorithm, as summarized in Algorithm 1. Given the channels \mathcal{F}_e , the optimal power allocation for user e , which transmits without any interference, is computed by means of (18). Subsequently, given the known values Γ_u , r_u and \mathcal{F}_u , and to compute the feasible power P_u , we consider the mRB experiencing the worst interference, denoted as

$$f^{\max} = \arg \max_f P_e(f). \quad (32)$$

Then, from the lookup table $\hat{p}_u(\cdot, P_e, \Gamma_u, \mathcal{F}_u, r_u)$, we obtain the minimum P_u that meets the outage probability constraint when the interference is given by $P_e(f^{\max})$, i.e.,

$$P_u = \min \{ P \mid \hat{p}_u(P, P_e(f^{\max}), \Gamma_u, \mathcal{F}_u, r_u) \leq \epsilon_u \}. \quad (33)$$

In other words, we found the feasible power needed for the transmission assuming that all channels experience the strongest interference. Finally, we set:

$$P_u^*(f) = \max \{P_u, P_u^{\text{SIC}}(f)\}, \quad \forall f \in \mathcal{F}_u. \quad (34)$$

The procedure is summarized in Algorithm 1. In the following, we show that this algorithm provides a feasible solution to the allocation process.

Proposition 2. *Algorithm 1 guarantees a feasible solution of OMA allocation problem (13) and NOMA allocation problem (14).*

Proof. The allocation found with Algorithm 1 meets all the constraints of problems (13) and (14) and such is a *feasible* solution. In fact constraints (13.a) and (14.a) are met by employing (18). Constraints (13.b) is satisfied by construction by virtue of orthogonal allocation. Constraints (13.c) and (14.c) are addressed by employing the lookup table as in (33) and, finally, (14.b) is met by choosing $P_u^*(f)$ as in (34) $\forall f \in \mathcal{F}_u$. \square

It is worth noting that this scheme is generally sub-optimal in terms of power spent, considering that we constrain all channels to act as the worst one. On the other hand, for OMA allocation, we can demonstrate the following proposition.

Proposition 3. *Given Γ_u , \mathcal{F}_u , and r_u , if the lookup table (31) contains an entry where $\hat{p}_u(P_u, 0, \Gamma_u, \mathcal{F}_u, r_u) = \epsilon_u$ exactly, Algorithm 1 provide the optimal solution of the URLLC OMA allocation problem (23), and the optimal power coefficient is $P_u^*(f) = P_u, \forall f \in \mathcal{F}_u$.*

Proof. See Appendix B. \square

In practical terms, Proposition 3 implies that the solution given by Algorithm 1 is reasonably close to the optimal one for the OMA allocation. The larger is the set of P_u values in the lookup table (31), the closer we get to the optimal results.

The computational complexity of Algorithm 1 depends on: the complexity of the water-filling algorithm, being $\mathcal{O}(F)$ for the single-user case [23, Proposition 1]; the complexity of the maximum operator, whose worst-case is $\mathcal{O}(F)$; the complexity of retrieving the minimum power from the lookup table, which is linear with the number of the element of the table involved in the power coefficient retrieval $\mathcal{O}(L^{\text{fea}})$. The total computational complexity is $\mathcal{O}(3F + L^{\text{fea}})$, where L^{fea} is generally the dominant term. It is worth noting that $L^{\text{fea}} \ll L$, and the former is equal to the number of P_u values tested in the lookup table, considering that the scheduler is previously informed of Γ_u, \mathcal{F}_u , and r_u . We remark that the initialization of the procedure is not considered because the computational load required for creating (31) can be performed offline. In other words, the population of the look-up table does not directly increase the complexity of the resolution of the URLLC allocation problem.

Algorithm 1: Feasible algorithm (N-fea)

- 1 **Initialize:** Populate the table $\hat{p}_u(P_u, P_e, \Gamma_u, \mathcal{F}_u, r_u)$;
 - 2 Compute \mathbf{P}_e through (18);
 - 3 Compute $\mathbf{P}_u^{\text{SIC}}$ through (20);
 - 4 $f^{\text{max}} = \arg \max_f P_e(f)$;
 - 5 $P_u = \min\{P_u \mid \hat{p}_u(P_u, P_e(f^{\text{max}}), \Gamma_u, \mathcal{F}_u, r_u) \leq \epsilon_u\}$;
 - 6 $P_u^*(f) = \max \{P_u, P_u^{\text{SIC}}(f)\}, \forall f \in \mathcal{F}_u$;
 - 7 **Output:** \mathbf{P}_u^*
-

4.3 Constrained block coordinated descent (BCD) optimization

To overcome the sub-optimality given by Algorithm 1, we propose an iterative algorithm based on BCD optimization, a class of algorithms able to effectively solve large-scale optimization problems [28]. The main idea is based on non-increasing property of the outage probability (21) given in Proposition 1.

We start from the solution given by Algorithm 1. For each iteration, we update the power coefficients one after another, following a deterministic order. Without loss of generality, we assume that the predetermined order is the natural order of set \mathcal{F}_u , i.e., $0, 1, 2, \dots, F_u - 1$. To take into account the dimension-wise updating

process, we denote the power coefficient vector at iteration i where the first $f \in \mathcal{F}_u$ terms have been updated as

$$\mathbf{P}_u^{(i,f)} = [P_u^{(i)}(0), \dots, P_u^{(i)}(f-1), P_u^{(i-1)}(f), \dots, P_u^{(i+1)}(F_u-1)]^T. \quad (35)$$

The aim is to update each power coefficient only if the resulting outage probability satisfies the reliability requirement. To guarantee the feasibility of using $\mathbf{P}_u^{(i,f)}$, the power coefficient of frequency component $f \in \mathcal{F}_u$ is updated as follows

$$P_u^{(i)}(f) = \begin{cases} \max \left\{ P_u^{\text{SIC}}(f), P_u^{(i-1)}(f) - \mu^{(i)} \right\}, & \text{if } \hat{p}_u(\mathbf{P}_u^{(i,f)}, \mathbf{P}_e, \Gamma_u, \mathcal{F}_u, r_u) \leq \epsilon_u, \\ P_u^{(i-1)}(f), & \text{otherwise,} \end{cases} \quad (36)$$

where $\mu^{(i)} > 0$ is the step size at iteration i , $\hat{p}_u(\mathbf{P}_u^{(i,f)}, \mathbf{P}_e, \Gamma_u, \mathcal{F}_u, r_u)$ is the Monte Carlo estimation of the outage probability setting as input vector $\mathbf{P}_u^{(i,f)}$. To avoid unnecessary computations, when a power coefficient reaches $P_u^{\text{SIC}}(f)$, the updating process for that frequency is not performed anymore. To assure the convergence near to the optimal solution, we halve the value of step size when the updating rule (36) lets the vector unchanged. Hence, the step size updating rule is

$$\mu^{(i)} = \begin{cases} \mu^{(i-1)}/2, & \text{if } \mathbf{P}_u^{(i,F_u)} = \mathbf{P}_u^{(i-1,F_u)} \\ \mu^{(i-1)}, & \text{otherwise.} \end{cases} \quad (37)$$

The algorithm stops when the step size is lower or equal to a certain threshold τ . The overall algorithm is summarized in Algorithm 2.

Taking into account that the objective function of (23) is monotonically non-decreasing, we can prove the following Proposition.

Proposition 4. *There exists a minimum value of the threshold τ for which Algorithm 2 provides the optimal solution for problem (23).*

Proof. See Appendix C. □

In theory, the optimal solution is guaranteed to be obtained only in the asymptotic behavior $\tau \rightarrow 0$. When the threshold tends to zero, the algorithm iterates until the border of the feasible set is found (see Appendix C). However, this leads to a number of iterations of the algorithm that tends to the infinite; hence, the algorithm cannot be implemented in this way. In practice, we can set τ as the minimum variation of power allowed at the BS to obtain the closest to the optimum solution.

The complexity of each iteration i of the BCD algorithm is dominated by the estimation of outage probability when applying update rule (36), i.e., $\mathcal{O}(nF_u)$ (see eq. (31)). Cycling through all the frequencies, the complexity for the iteration i is in the worst case $\mathcal{O}(nF_u^2)$. Denoting the number of iterations as a function of the threshold as $I(\tau)$, we have a total complexity of $\mathcal{O}(nF_u^2I(\tau))$. Even setting a τ to provide a low number of iterations, the dominant term remains n , which needed to be a high value to obtain an accurate estimation of the outage probability. Therefore, this algorithm can be hardly used in a real scenario, but it represents a good benchmark for evaluating the performance of the NOMA approach.

Algorithm 2: Constrained BCD (N-BCD)

- 1 **Initialize:** $\mu^{(0)} > 0$, Compute \mathbf{P}_e from (18), $\mathbf{P}_u^{(0,F_u)}$ using Algorithm 1; $i \leftarrow 1$, $\mathcal{F}^+ \leftarrow \mathcal{F}_u$;
 - 2 **while** $\mu^{(i)} > \tau$ **do**
 - 3 **for** $f \in \mathcal{F}^+$ **do**
 - 4 Update $P_u^{(i)}(f)$ using (36);
 - 5 **if** $P_u^{(i)}(f) \geq P_u^{\text{SIC}}(f)$ **then**
 - 6 $\mathcal{F}^+ \leftarrow \mathcal{F}^+ \setminus \{f\}$
 - 7 $i \leftarrow i + 1$;
 - 8 Update $\mu^{(i)}$ using (37)
 - 9 **Output:** $\mathbf{P}_u^* \leftarrow \mathbf{P}_u^{(i-1,F_u)}$
-

5 Numerical results

In this Section, the performance comparison between OMA and NOMA for spectrum slicing of eMBB and URLLC traffic is presented. In the absence of other literature on the subject, our focus is to investigate in depth the various effects that play a role in the computation of the power consumption, such as channel diversity, interference cancellation, and URLLC requirements. We consider a resource grid formed by $F = 12$ frequencies and $M = 7$ mini-slots. We consider that the time of a slot is $T = 1$ ms, obtaining $T_m = T/M = 1/7$ ms as the minimum URLLC time slot of the 5G NR standard [1]. Finally, each mRB has bandwidth $\Delta_f = 180$ kHz.

The reliability requirement of URLLC user is set as $\epsilon_u = 10^{-5}$. The fading channels for both users are Rayleigh distributed with scale parameter $\sqrt{\Gamma_i}$, $i \in \{e, u\}$. In the Monte Carlo simulation used to obtain the lookup table (31), we vary the powers P_i , $i \in \{e, u\}$ of each mRB from -30 dBm to 30 dBm per mRB, with granularity 1 dBm.

For each instance of simulation, we place the users in a cell of 500 m in radius and we compute the power consumption using both OMA and NOMA. The distance d_i , $i \in \{e, u\}$ of the users from the BS is computed by inverting the well-known wireless path loss formulation, i.e., $d_i = \sqrt[\psi]{10^{G/10} L_i \left(\frac{c}{f_0 4\pi}\right)^2 d_0^{\psi-2}}$, where $G = 17.15$ dB is the overall antenna gain of BS and user; $f_0 = 2$ GHz is the central working frequency; c is the speed of light; $d_0 = 10$ m is the free-space region of the cell near to the BS; $\psi = 4$ is the path loss exponent; $L_i = \sigma^2/\Gamma_i$ is the path loss. We set the receiver noise as $\sigma^2 = -108$ dBm.

In the case of NOMA, we show the results of Algorithms 1 and 2, labeled as N-fea and N-BCD, respectively. For this paradigm, we always present the results obtained setting $F_u = F = 12$. We remark that the choice of this parameter does not influence the eMBB allocation while increasing the number of resources available reduces the power coefficients needed for SIC (see (20)). We set the threshold of the BCD approach as $\tau = 10^{-7}$. In the case of OMA, we present the results for different frequencies reserved for the URLLC data stream transmission. In particular, we set $F_u \in \{3, 6, 9\}$, labeled as O-3, O-6, O-9, respectively. To correctly compare the performance of schemes with different number of resources available, we fix the number of bits to be transmitted in the whole slot as $N_e = 8640$ and $N_u = \frac{2160}{7}$. In this way, the spectral efficiency for NOMA with $M_u = 1$ are $r_u = 1$ bit/s/Hz and $r_e = 4$ bit/s/Hz. For the other M_u values, the spectral efficiencies can be computed through (2).

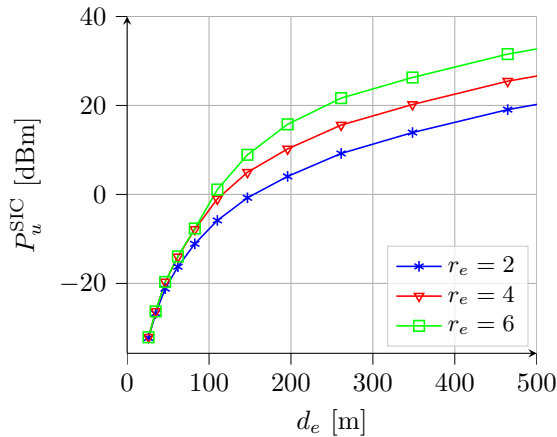


Figure 4: Average power consumption required by SIC as a function of d_e , $F_u = 12$.

Firstly, we study the behavior of the power needed for the SIC process given in eq. (20). Fig. 4 shows the overall power required for the SIC process $P_u^{\text{SIC}} = \sum_{f \in \mathcal{F}_u} P_u^{\text{SIC}}(f)$ as a function of the distance of the eMBB user d_e . As expected, the closer the eMBB user to the BS the smaller the power needed for the SIC. We can also see that the gap between different spectral efficiencies starts to be relevant when $d_e \geq 100$ m. For higher distances, increasing the spectral efficiency increases the value of eMBB power \mathbf{P}_e given by solution (18); for lower distances, the evaluated power is dominated by the terms $1/\gamma_e(f)$. We remark that a low d_e means a high average SNR Γ_e leading to a higher probability of having high values of $\gamma_e(f)$.

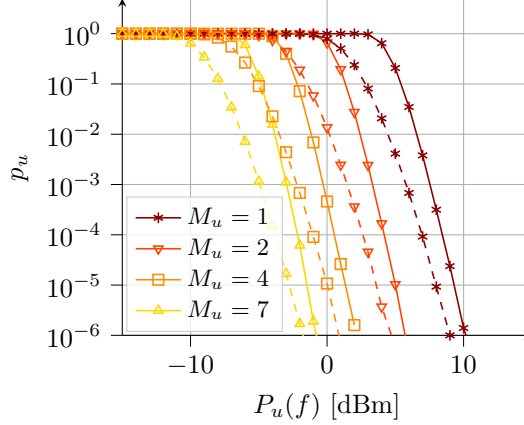


Figure 5: Outage probability p_u versus $P_u(f)$, for $\Gamma_u = 30$ dB, $F_u = 12$ and different M_u . $P_u(f) = P_u$, $P_e(f) = P_e, \forall f \in \mathcal{F}_u$. The solid lines are for $P_e(f) = 0$ dBm while dashed lines represent $P_e(f) = -\infty$ dBm, i.e., no interference.

In the following, we show the effect of the URLLC transmission time M_u on the power allocation. Fig. 5 shows the outage probability p_u as a function of the power $P_u(f)$, when all transmitting and interference power coefficients are the same for each mRB, i.e., $P_u(f) = P_u$, $P_e(f) = P_e, \forall f \in \mathcal{F}_u$, $\Gamma_u = 30$ dB, and $F_u = 12$. The dashed lines are the outage probability curves with no interference, i.e. $P_e = -\infty$ dBm, while the solid lines represent the outage probability with $P_e = 0$ dBm. We present different plots for different M_u . Increasing the value of M_u , will reduce the spectral efficiency r_u leading to a reduction of the power needed to meet the target outage probability ϵ_u . Therefore, the best solution is design a system able to exploit the whole latency requirement. Having shown this result, we will focus only on the results of $M_u = 1$ in the remainder of the Section, remarking that increasing M_u reduces the overall power spent for all the schemes presented.

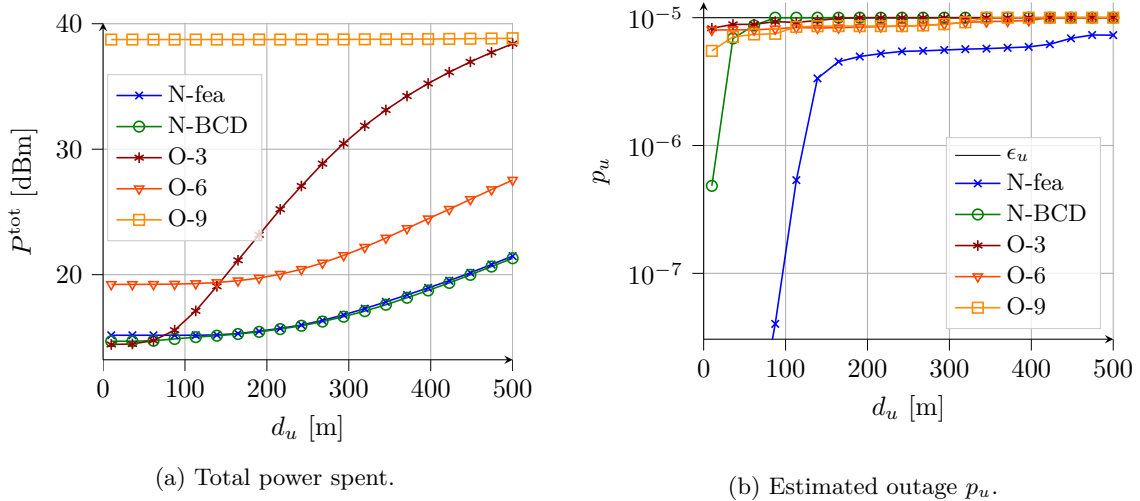
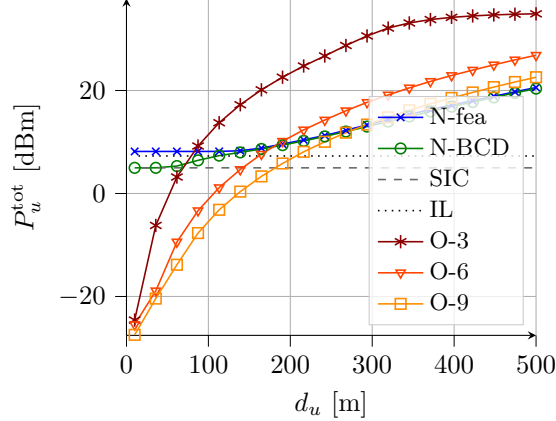


Figure 6: Average results obtained as a function of URLLC distance d_u , $d_e = 146.9$ m.

Fig. 6a shows the total power spent P^{tot} as a function of d_u , when user e is placed at $d_e = 146.9$ m (corresponding to $\Gamma_e = 50$ dB). We can see that N-fea and N-BCD assure a lower power consumption than the OMA paradigms, as soon as $d_u \geq 75$ m. N-BCD performs better than OMA schemes also for $d_u \geq 65$ m. The performance gap between N-BCD and N-fea is negligible for every value of d_u under analysis. On the other hand, the OMA paradigm performs slightly better on short distances, i.e., $d_u < 65$ m. In particular, the best results in a high SNR regime are attained by O-3. Moreover, Fig. 6b presents the corresponding estimated p_u , evaluated with the allocated power coefficients \mathbf{P}_u and \mathbf{P}_e , while the channel gains of u are randomly generated. For the OMA schemes, the target outage is met, guaranteeing $p_u \leq \epsilon_u$. The slight differences from the target outage for short distances are due to the quantization of power available

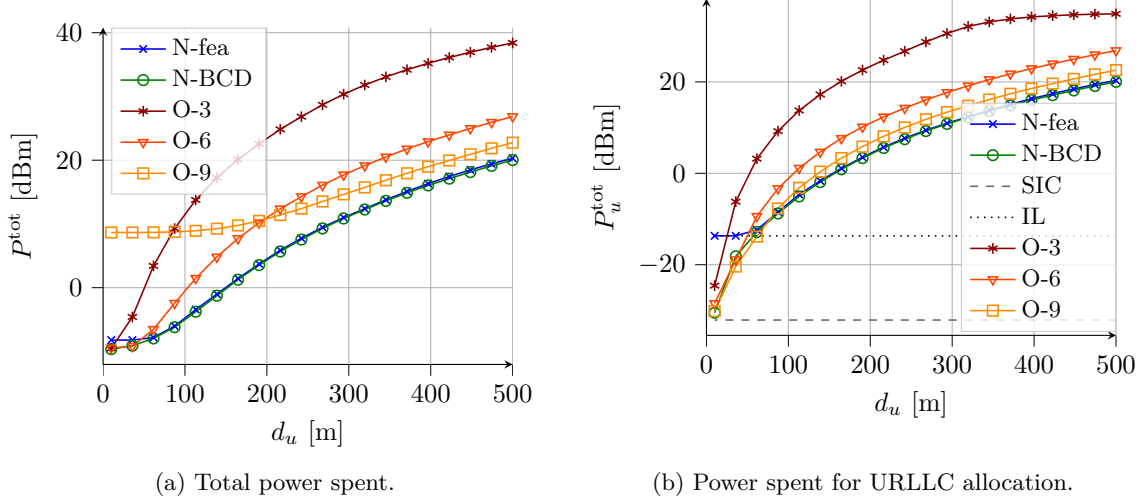
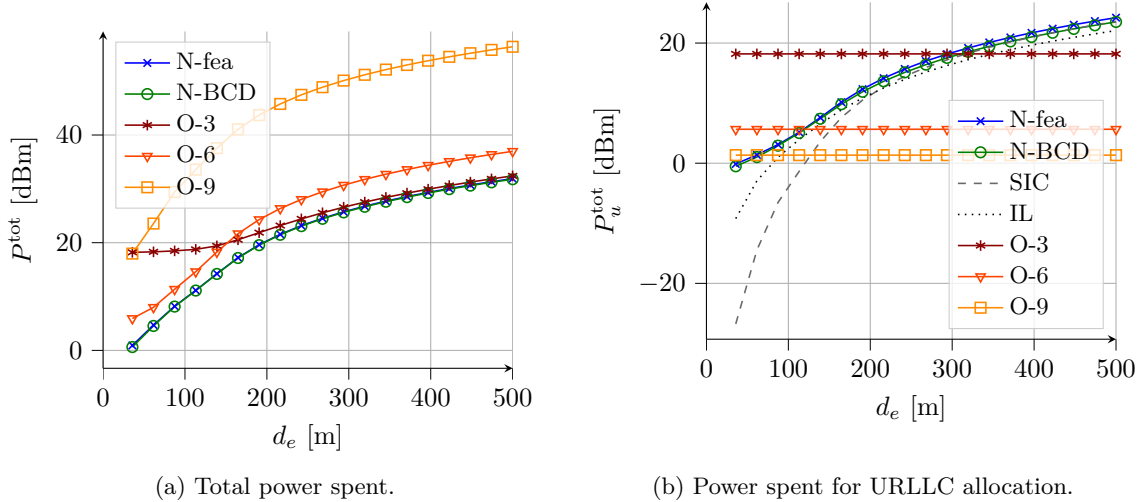

 Figure 7: Average URLLC power spent as a function of d_u , $d_e = 146.9$.

in the lookup table solution, set as 1 dB. The outage probability of N-fea is always lower than ϵ_u , proving that this scheme provides a feasible but not optimal solution. On the other hand, N-BCD reaches exactly the target outage probability until $d_u \geq 85$ m. For shorter distances, the power allocation is dominated by the SIC process limiting the minimum power needed, as we will see in the following.

To explain the (slight) superiority of OMA to NOMA for small d_u -or high Γ_u regime-, we present the power needed for URLLC and eMBB requirements separately. In Fig. 7, we plot the power spent for the URLLC user $P_u^{\text{tot}} = \sum_{f \in \mathcal{F}_u} P_u(f)$. In this figure, we show the power allocated using the various NOMA and OMA paradigms, as well as the power needed by the SIC process (20), namely SIC, and the power bound of the interference-limited scenario (30), namely IL. It is worth noting that these last two results depend on the eMBB power only. The powers spent for the NOMA schemes are dominated by different effects for short distances. For N-fea, the interference-limited bound is the minimum power achievable. We remark that the power computed by (34) is obtained assuming that all the channels experience the maximum interference. Hence, the mutual information achievable using the power coefficient given by N-fea tends to the approximation (28) on closer distances. On the other hand, N-BCD naturally exploits also the channels with no interference, enabling the possibility of reaching the power needed for the SIC process, which is the lower limit of the NOMA approach. It is worth noting that even a small increment of URLLC power employed leads to a considerable reduction of the outage probability (see Fig. 6) due to the non-linear relation between these quantities. For the OMA schemes, the power spent decreases when resources reserved for the URLLC increase. For short distances, these schemes may consume less power w.r.t. NOMA due to the lack of interference and lower limits. We remark that the frequency diversity gain provided for very short distances ($d_u < 35$ m) is negligible w.r.t. to the gain given by the mean SNR, resulting in comparable performances for the three OMA schemes. Finally, in Table 1, we present the average power spent for the eMBB. Here, the two NOMA schemes are not presented because the eMBB power allocation is the same for both N-fea and N-BCD. From the table, we can infer that the eMBB power plays the dominant role in the power allocation, explaining why O-9 total power is almost flat in Fig. 6a, even if it can benefit from the lowest URLLC power consumption. The same consideration can be made also for O-6. However, O-3 and NOMA have comparable performance, and the best allocation scheme depends only on the URLLC power consumption for $d_e \geq 146.9$, clarifying the results obtained in Fig. 6.

Table 1: Average eMBB power spent in dBm.

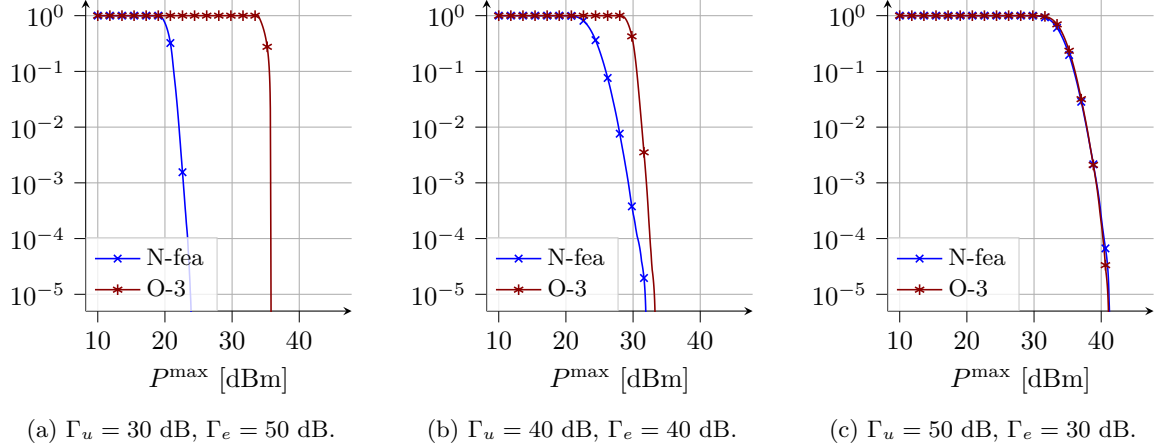
Γ_e [dB]	d_e [m]	NOMA	O-3	O-6	O-9
30	464.56	33.21	34.18	38.89	58.27
40	261.2	23.36	24.32	29.09	48.54
50	146.9	14.21	14.44	19.23	38.74
60	82.6	5.84	5.84	9.05	28.44
70	46.5	-1.87	-1.87	-0.64	18.79
80	26.1	-9.67	-9.67	-9.67	8.65


 Figure 8: Average results obtained as a function of URLLC distance d_u , $d_e = 26.1$ m.

 Figure 9: Average results obtained as a function of eMBB distance d_e , $d_u = 146.9$ m.

In Fig. 8, we present the power results in the extreme case of $d_e = 26.1$ m. In this case, the allocated eMBB power is low, and it is the same for NOMA, O-3, and O-6, as shown in Table 1. With this power allocation, the N-BCD approach is never limited by the SIC, and its performances are the best for every value of d_u . Note that in this extreme case, the best performances between the OMA schemes are attained by O-6, which consumes the same eMBB power but benefits from the frequency diversity gain for URLLC allocation.

In Fig. 9, we show the power spent as a function of d_e , fixing $d_u = 146.9$ m. In detail, Fig. 9a shows the overall power spent; also in this case, the NOMA schemes attain the best performance. Fig. 9a shows the URLLC power spent to meet the reliability requirement. In this case, the OMA power does not change for the different values of d_e , having fixed d_u . On the contrary, NOMA URLLC power is still influenced by the interference given by P_e , and thus P_u^{tot} increases when d_e increases, accordingly.

Finally, Fig. 10 shows the impact of considering the BS power budget P^{max} for N-fea and O-3. We plot the probability that the total power allocated is higher than the power budget, i.e., $\Pr\{P^{\text{tot}} > P^{\text{max}}\}$, varying the latter, and with different combinations of Γ_u and Γ_e . The NOMA approach can provide better performance if $\Gamma_u \leq \Gamma_e$, i.e., when the eMBB is the *strong* user, accordingly with the imposition of employing the SIC process at such user.


 Figure 10: Probability of outage due to the power budget, for different value of Γ_e and Γ_u .

6 Conclusions and future directions

This paper studied the power and resource allocation for the downlink communication spectrum slicing of eMBB and URLLC traffic. We focused on orthogonal and non-orthogonal multiple access schemes employing the parallel channel model. Due to the nature of the communication traffic types, we assumed that the CSI is only statistical for the URLLC, while the eMBB channel relies on instantaneous information. We proposed a feasible and a BCD algorithm able to solve the spectrum slicing problem by minimizing the power spent, assuring at the same time the requirements of both kinds of traffic. We also compared the impact of using the aforementioned multiple access scheme for a 5G-like resource grid available. Numerical results showed that the NOMA paradigm attains the best performance in almost all cases. The only exception is for a very close URLLC user, where the frequency diversity gain is negligible. In that case, OMA could attain the best performance depending on the position of the eMBB user. However, the performance gain w.r.t. NOMA is still negligible, proving that NOMA is a promising technology for spectrum slicing. We also proved experimentally that the lookup table algorithm provides a close-to-the-optimal power allocation, becoming a possible candidate for a practical resource allocation approach.

This work is a first step to understanding the optimal design of a beyond 5G network enabling spectrum slicing on downlink communications. Based on our promising results and insights, our future work will investigate spectrum slicing in a more practical scenario with several users for the two types of traffic, considering both single-antenna and multiple-antenna technologies.

A Proof of Proposition 1

The log function is monotonic non-decreasing w.r.t. each $P_u(f)$. If we consider the vector \mathbf{P}'_u obtained decreasing $P_u(f)$, $f \in \mathcal{F}_u$, by $\delta > 0$, while the other $P_u(g)$, $\forall g \in \mathcal{F}_u \setminus \{f\}$, and $P_e(j)$, $\forall j \in \mathcal{F}_u$, are kept the same, the mutual information results

$$F_u I_u(\mathbf{P}'_u) = \log_2 \left(1 + \frac{\gamma_u(f)(P_u(f) - \delta)}{1 + \gamma_u(f)P_e(f)} \right) + \sum_{g \in \mathcal{F}_u \setminus \{f\}} \log_2 \left(1 + \frac{\gamma_u(f)P_u(f)}{1 + \gamma_u(f)P_e(f)} \right) \leq F_u I_u(\mathbf{P}_u).$$

Therefore, the outage probability may only result larger (or equal), i.e., $p_u(\mathbf{P}'_u) = \Pr\{I_u(\mathbf{P}'_u) \leq r_u\} \geq p_u(\mathbf{P}_u) = \Pr\{I_u(\mathbf{P}_u) \leq r_u\}$. The same relation is in fact extended for each $\mathbf{0} \leq \mathbf{P}'_u \leq \mathbf{P}_u$, which completes the proof. \square

B Proof of Proposition 3

For the OMA allocation, the power coefficient of e user is zero for every resources given to u , i.e. $P_e(f) = 0$, $\forall f \in \mathcal{F}_u$. In these conditions of i.i.d. parallel channels without interference, the minimum outage probability is reached when the same power coefficient is allocated to each channel [21]. As a matter of fact, Algorithm 1 outputs the power coefficient P_u given by (33) for each mRB, due to the lack of SIC constraint. The resulting

vector $\mathbf{P}_u^* = [P_u, \dots, P_u]^T$ is at least a feasible solution of problem (13), due to Proposition 2. The resulting mutual information is $I_u(\mathbf{P}_u^*, \mathbf{P}_e) = I_u(P_u, 0) = \frac{1}{F_u} \sum_{f \in \mathcal{F}_u} \log_2(1 + \gamma_u(f)P_u)$. Following Proposition 1, the outage probability $p_u(\mathbf{P}_u^*)$ is monotonically non-increasing in P_u . Having obtained P_u from (33), there is no other power coefficient $P'_u \leq P_u$ such as $\hat{p}_u(P'_u, 0, \Gamma_u, \mathcal{F}_u, r_u) \leq \epsilon_u$. If the table has been populated with enough different values of P_u , we will find that $p_u(P_u, 0, \Gamma_u, \mathcal{F}_u, r_u) = \epsilon_u$, and the optimal solution is reached. \square

C Proof of Proposition 4

The objective function of problem (23) is a non-decreasing function with gradient equal to $\mathbf{1}$. Hence, no saddle point can be found and the optimal solution lay on the border of the feasible set [29]. The power updating rule (36) guarantees that the magnitude of vector \mathbf{P}_u decreases at every iteration, following the minimization direction. Let us suppose that the optimal solution is \mathbf{P}_u^o , and the Algorithm has stopped on point \mathbf{P}_u^* when the threshold is set as τ' . If $\mathbf{P}_u^o = \mathbf{P}_u^*$, the proof is completed. Let us now assume that the vector \mathbf{P}_u^* has the same optimal coefficients except for one dimension f , i.e. $P_u^o(f) < P_u^*(f)$, and $P_u^o(g) = P_u^*(g) \forall g \in \mathcal{F}_u \setminus \{f\}$. This means that there exists a feasible point on dimension $f \in \mathcal{F}_u$ that will provide a smaller objective function. Hence, considering $\tau'' < \tau'$, using both (37) and (36), it is possible to reduce $P_u^*(f)$ toward $P_u^o(f)$. Reducing τ'' , there exists a value of the threshold $0 < \tau^* \leq \tau''$ such as updating rules (37) and (36) will provide exactly $P_u^o(f)$. The same results can be extended for the general case where \mathbf{P}_u^o and \mathbf{P}_u^* differ by more than one element, completing the proof. \square

References

- [1] 3GPP, “Study on New Radio (NR) access technology,” 3rd Generation Partnership Project (3GPP), Technical Report (TR) 38.912, 05 2017, version 14.0.0.
- [2] H. Zhang, N. Liu, X. Chu, K. Long, A. H. Aghvami, and V. C. M. Leung, “Network slicing based 5G and future mobile networks: Mobility, resource management, and challenges,” *IEEE Commun. Mag.*, vol. 55, no. 8, pp. 138–145, 2017.
- [3] S. D’Oro, F. Restuccia, A. Talamonti, and T. Melodia, “The slice is served: Enforcing radio access network slicing in virtualized 5G systems,” in *IEEE INFOCOM 2019*, 2019, pp. 442–450.
- [4] A. Anand, G. de Veciana, and S. Shakkottai, “Joint scheduling of URLLC and eMBB traffic in 5G wireless networks,” *IEEE/ACM Trans. Netw.*, vol. 28, no. 2, pp. 477–490, 2020.
- [5] M. Elsayed and M. Erol-Kantarci, “AI-Enabled Radio Resource Allocation in 5G for URLLC and eMBB Users,” in *2019 IEEE 5GWF*, 2019, pp. 590–595.
- [6] M. Alsenwi, N. H. Tran, M. Bennis, S. R. Pandey, A. K. Bairagi, and C. S. Hong, “Intelligent resource slicing for eMBB and URLLC coexistence in 5G and beyond: A deep reinforcement learning based approach,” *IEEE Trans. Wireless Commun.*, pp. 1–1, 2021.
- [7] Y. Huang, Y. T. Hou, and W. Lou, “DELUXE: A DL-based link adaptation for URLLC/eMBB multiplexing in 5G NR,” *IEEE Journal on Selected Areas in Communications*, vol. 40, no. 1, pp. 143–162, 2022.
- [8] P. Xu, Z. Ding, X. Dai, and H. V. Poor, “NOMA: an information theoretic perspective,” *CoRR*, vol. abs/1504.07751, 2015.
- [9] P. Popovski, K. F. Trillingsgaard, O. Simeone, and G. Durisi, “5G wireless network slicing for eMBB, URLLC, and mMTC: A communication-theoretic view,” *IEEE Access*, vol. 6, pp. 55 765–55 779, 2018.
- [10] A. E. Kalør and P. Popovski, “Ultra-reliable communication for services with heterogeneous latency requirements,” in *2019 IEEE Globecom Workshops*, 2019, pp. 1–6.
- [11] Y. Li, C. Hu, J. Wang, and M. Xu, “Optimization of URLLC and eMBB multiplexing via deep reinforcement learning,” in *2019 IEEE ICC Workshops*, 2019, pp. 245–250.
- [12] F. Chiariotti, I. Leyva-Mayorga, C. Stefanović, A. E. Kalør, and P. Popovski, “Spectrum slicing for multiple access channels with heterogeneous services,” *Entropy*, vol. 23, no. 6, 2021.
- [13] Z. Wei, D. W. K. Ng, J. Yuan, and H.-M. Wang, “Optimal resource allocation for power-efficient MC-NOMA with imperfect channel state information,” *IEEE Transactions on Communications*, vol. 65, no. 9, pp. 3944–3961, 2017.

- [14] F. Yilmaz and M.-S. Alouini, "Outage capacity of multicarrier systems," in *2010 17th International Conference on Telecommunications*, 2010, pp. 260–265.
- [15] B. Bai, W. Chen, K. B. Letaief, and Z. Cao, "Outage exponent: A unified performance metric for parallel fading channels," *IEEE Trans. Inf. Theory*, vol. 59, no. 3, pp. 1657–1677, 2013.
- [16] J. P. Coon, D. E. Simmons, and M. D. Renzo, "Approximating the outage probability of parallel fading channels," *IEEE Commun. Lett.*, vol. 19, no. 12, pp. 2190–2193, 2015.
- [17] C. She, C. Yang, and T. Q. S. Quek, "Radio resource management for Ultra-Reliable and Low-Latency Communications," *IEEE Commun. Mag.*, vol. 55, no. 6, pp. 72–78, 2017.
- [18] Y. Polyanskiy, H. V. Poor, and S. Verdú, "Channel coding rate in the finite blocklength regime," *IEEE Trans. Inf. Theory*, vol. 56, no. 5, pp. 2307–2359, 2010.
- [19] W. Yang, G. Durisi, T. Koch, and Y. Polyanskiy, "Quasi-static multiple-antenna fading channels at finite blocklength," *IEEE Trans. Inf. Theory*, vol. 60, no. 7, pp. 4232–4265, 2014.
- [20] G. Durisi, T. Koch, and P. Popovski, "Toward massive, ultra reliable, and low-latency wireless communication with short packets," *Proc. IEEE*, vol. 104, no. 9, pp. 1711–1726, 2016.
- [21] D. Tse and P. Viswanath, *Fundamentals of Wireless Communication*. USA: Cambridge University Press, 2005.
- [22] S. Li, M. Derakhshani, S. Lambotharan, and L. Hanzo, "Outage probability analysis for the multi-carrier NOMA downlink relying on statistical CSI," *IEEE Trans. Commun.*, vol. 68, no. 6, pp. 3572–3587, 2020.
- [23] D. Palomar and J. Fonollosa, "Practical algorithms for a family of waterfilling solutions," *IEEE Trans. Signal Process.*, vol. 53, no. 2, pp. 686–695, 2005.
- [24] P. He, L. Zhao, S. Zhou, and Z. Niu, "Water-filling: A geometric approach and its application to solve generalized radio resource allocation problems," *IEEE Trans. Wireless Commun.*, vol. 12, no. 7, pp. 3637–3647, 2013.
- [25] L. P. Qian, Y. J. Zhang, and J. Huang, "MAPEL: Achieving global optimality for a non-convex wireless power control problem," *IEEE Trans. Wireless Commun.*, vol. 8, no. 3, pp. 1553–1563, 2009.
- [26] M. Jaggi, "Revisiting Frank-Wolfe: Projection-free sparse convex optimization," in *Proceedings of the 30th International Conference on Machine Learning - Volume 28*, ser. ICML'13. JMLR.org, 2013, p. I–427–I–435.
- [27] X. Wang, J. Wang, L. He, and J. Song, "Outage analysis for downlink NOMA with statistical channel state information," *IEEE Wireless Commun. Lett.*, vol. 7, no. 2, pp. 142–145, 2018.
- [28] Y. Xu and W. Yin, "A globally convergent algorithm for nonconvex optimization based on block coordinate update," *J. Sci. Comput.*, vol. 72, no. 2, pp. 700–734, 2017.
- [29] S. Boyd and L. Vandenberghe, *Convex Optimization*. Cambridge University Press, 2004.